Application of a pseudo-one-dimensional kinetic Ising model to proton spin-lattice relaxation rates in squaric acid ($H_2C_4O_4$)

U. Deininghaus,* H. Fischer,† P. K. Kahol, and M. Mehring
Physikalisches Institut 2, Universität Stuttgart, 7000 Stuttgart 80, Federal Republic of Germany
(Received 4 June 1984)

A kinetic model of three-dimensionally-coupled Ising chains is applied to study the proton spin-lattice relaxation rates in $H_2C_4O_4$. Good agreement with the experimental proton spin-lattice relaxation rates implies the validity of the model in visualizing $H_2C_4O_4$ as a quasi-one-dimensional solid.

I. INTRODUCTION

Squaric acid ($H_2C_4O_4$) is a molecular solid which shows a structural first-order antiferrodistortive phase transition[1–4] at $T_c=373$ K from a tetragonal (high-temperature phase) to a monoclinic structure (low-temperature phase). The corresponding universality class in renormalization-group language is $n=2$, $d=3$ where n is the number of order-parameter components and d is the dimensionality. The relevant mechanism for the phase transition is accompanied by the order-disorder behavior of protons. We do not, however, propose that the protons alone are driving the phase transition, but believe that the high polarizability of the C_4O_4 unit plays a significant part in the structural change, as was recently established by ^{13}C NMR measurements.[5] The structural information of this solid prompted us earlier to propose a model of three-dimensionally-coupled Ising chains.[6] In order to visualize this chain structure we have plotted in Fig. 1 a single ac plane of squaric acid with two orthogonal chains being emphasized. The model is a hydrogen-bond chain network, consisting of parallel chains with strong coupling J_1 in the chain direction and much weaker coupling J_2 between parallel chains. Parallel to the *ac* plane and along the *b* direction there are other layers stacked with a separation $b/2$. J_3 represents the coupling to such neighboring layers. These three coupling constants were found[6] to be $J_1=149$ K, $J_2=63$ K, and $J_3=-5$ K in the mean-field approximation of a one-dimensional chain by fitting to the neutron scattering data of Samuelsen and Semmingsen.[2(b)] Due to the fact that the intrachain coupling is much larger than all other coupling constants, one can justifiably treat one chain rigorously and incorporate the interchain interactions through, e.g., mean-field approximation. Such models have been used with fairly good success in investigating the static as well as dynamic properties of molecular solids.[7–11]

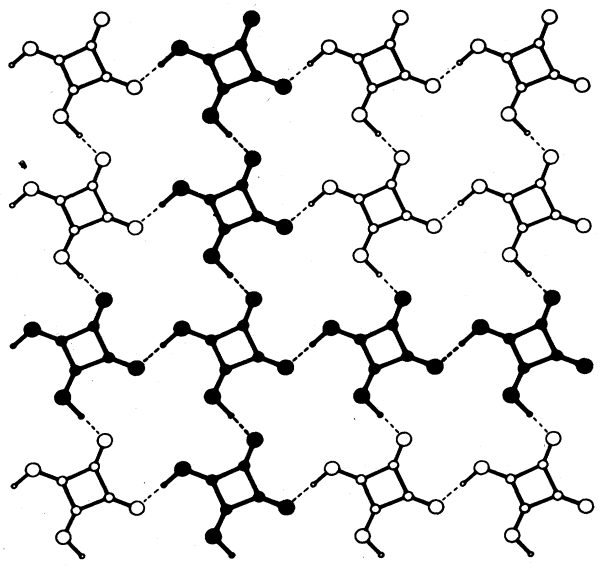

FIG. 1. ac plane of squaric acid with two orthogonal chains being emphasized to suggest the chainlike structure of this solid.

In this paper, our interest is in the chain dynamics which causes proton spin relaxation. One of the simplest models to study the dynamical cooperative phenomena is the Ising spin model, which, in an external magnetic field, has been solved by Žumer[10] for its kinetics. Since squaric acid can be visualized as a highly "one-dimensional solid" we can use the kinetic model to investigate the proton spin-lattice relaxation rate. We shall, however, give general results for the dynamical susceptibility which reduce to those of Žumer in certain approximations.

Before proceeding we should remark that proton spin-lattice relaxation measurements have been recently reported by Maier and Petersson.[12] These authors did, however, interpret their data in a classical way. Our data are in agreement with theirs in those cases where similar frequencies and orientations have been used.

II. BASIC THEORETICAL DETAILS

The spin-lattice relaxation rate, caused by fluctuating dipolar interactions and represented by the interaction Hamiltonian

$$\mathscr{H}_{\text{dipolar}}(t)=\sum_{i<j}\sum_{k=-2}^{2}F_{ij}^{(k)}(t)A_{ij}^{(k)}\,, \tag{1}$$

is given by[13]

$$\frac{1}{T_1}=3\gamma^4\hbar^2 I(I+1)\frac{1}{N}[J^{(1)}(\omega_0)+J^{(2)}(2\omega_0)] . \quad (2)$$

In the above equations $F^{(k)}$ are the lattice functions, $A^{(k)}$ are operators acting on spin variables, and the $J^{(k)}(\omega_k)$ are the spectral densities of the fluctuating dipolar tensor defined as

$$J^{(k)}(\omega_k)=\sum_{i<j}\int_{-\infty}^{\infty}d\tau e^{-i\omega_k\tau}\langle \Delta F_{ij}^{(k)}(0)\Delta F_{ij}^{(-k)}(\tau)\rangle , \quad (3)$$

where $\Delta F_{ij}^{(k)}(t)=F_{ij}^{(k)}(t)-\langle F_{ij}^{(k)}\rangle$, the angular brackets denoting the ensemble average.

In the pseudo spin picture, where a spin exists either in the right $(+1)$ or left (-1) equilibrium site, the variation of $F_{ij}^{(k)}$ with time can be represented through the ansatz[7]

$$F_{ij}^{(k)}(t)=C_{ij}^{(k)}+D_{ij}^{(k)}\sigma_i(t)+E_{ij}^{(k)}\sigma_j(t)+G_{ij}^{(k)}\sigma_i(t)\sigma_j(t) . \quad (4)$$

The last term, however, can be shown to be too small to retain. With the introduction of the Fourier components of $\sigma_i(t)$,

$$\sigma_i(t)=N^{-1/2}\sum_{\vec{q}}\sigma_{\vec{q}}(t)e^{i\vec{q}\cdot\vec{r}_i} , \quad (5)$$

the spectral densities in the continuum limit are written as

$$J^{(k)}(\omega_k)=\frac{V}{(2\pi)^3}\int d^3q[D+E+2DE(\vec{q})]S(\vec{q},\omega_k) , \quad (6)$$

where

$$D=\sum_j |D_{ij}|^2 , \quad (7)$$

$$E=\sum_j |E_{ij}|^2 , \quad (8)$$

$$DE(\vec{q})=\sum_j D_{ij}E_{ij}^{*}e^{i\vec{q}\cdot\vec{r}_{ij}} . \quad (9)$$

In obtaining the result (6), we have replaced the $\vec{q}$ summation by $\vec{q}$ integration which is to be performed over the Brillouin zone. V is the volume of the unit cell and $S(\vec{q},\omega)$ is the Fourier transform of the correlation function

$$S(q,t)=\langle\sigma_q(t)\sigma_{-q}(0)\rangle-\langle\sigma_q(0)\rangle\langle\sigma_{-q}(0)\rangle .$$

Using the fluctuation-dissipation theorem, the spectral densities are further expressed in terms of the imaginary part of the generalized dynamical susceptibility $\chi(\vec{q},\omega)$ which can be calculated for our system using the kinetic Ising model described by the Hamiltonian

$$\mathcal{H}=\sum_{\alpha=1}^{2}\left[J_1\sum_{i,j}\sigma_i^\alpha\sigma_j^\alpha+J_2\sum_{i,k}\sigma_i^\alpha\sigma_k^\alpha+J_3\sum_{i,l}\sigma_i^\alpha\sigma_l^\alpha\right] , \quad (10)$$

where the summation is performed over the two orthogonal sets of Ising chains.

In the mean-field approximation, which amounts to introducing the interchain couplings in the exact one-dimensional (1D) solution of the Ising Hamiltonian, the expression for $\chi^\alpha(\vec{q},\omega)$ is given by

$$\chi^\alpha(\vec{q},\omega)=\frac{\chi^\alpha(\vec{q},0)}{1+i\omega\tau_q^\alpha} , \quad (11)$$

where

$$\tau_q^\alpha=\frac{\tau_{q,1D}^\alpha}{1-\chi_{1D}^\alpha(\vec{q},0)J_\perp^\alpha(q)} , \quad (12)$$

$$\chi^\alpha(\vec{q},0)=\frac{\chi_{1D}^\alpha(\vec{q},0)}{1-\chi_{1D}^\alpha(\vec{q},0)J_\perp^\alpha(q)} , \quad (13)$$

with

$$\tau_{q,1D}^\alpha=\frac{\tau(1+X^2)}{1+X^2-2X\cos(\vec{q}_\alpha\cdot\vec{r}_\alpha)} , \quad (14)$$

$$\chi_{1D}^\alpha(\vec{q},\omega)=\beta(1-\langle\sigma\rangle^2)\frac{1-X^2}{1+X^2-2X\cos(\vec{q}_\alpha\cdot\vec{r}_\alpha)+i\omega\tau} , \quad (15)$$

$$X=\frac{\cosh(\beta h_{\rm eff})-[\sinh^2(\beta h_{\rm eff})+e^{-4\beta J_1}]^{1/2}}{\cosh(\beta h_{\rm eff})+[\sinh^2(\beta h_{\rm eff})-e^{-4\beta J_1}]^{1/2}} . \quad (16)$$

In expressions (11)–(16) τ is the flip time of each spin, $\langle\sigma\rangle$ is the order parameter, $\beta=(k_BT)^{-1}$, $h_{\rm eff}=(2J_2+8|J_3|)\langle\sigma\rangle$, and $J_\perp(q)$ is the Fourier component of the interchain interactions. The results of Žumer[10] are obtainable from the above expressions when the terms of order $h_{\rm eff}^2$ are neglected and $e^{-4\beta J_1}$ is assumed to be negligibly small. For $\alpha=1$, $\vec{q}_1\cdot\vec{r}_1=2\pi h$ and therefore

$$J_\perp^1(h,k,l)=2J_2\cos(2\pi l)+8J_3\cos(\pi h)\cos(\pi k)\cos(\pi l)$$

and for $\alpha=2$, $\vec{q}_2\cdot\vec{r}_2=2\pi l$ and $J_\perp^2(h,k,l)=J_\perp^1(l,k,h)$. Thus, the spin-lattice relaxation rate can be calculated from the above equations, the computational details of which are given in the next section.

III. RESULTS

The proton spin-lattice relaxation times T_1 were obtained with a Bruker SXP spectrometer, operating at 270 MHz, in pure single crystals of squaric acid for different temperatures ($288\le T\le 413$ K). The saturation-recovery method was employed and the relaxation behavior was found to be exponential. The crystal was oriented at three orientations, viz., $\theta=0°$, 54.7°, and 90° where θ is the angle between the static field $\vec{B}_0$ and the b axis. In the first orientation, the field was perpendicular to the chain whereas for $\theta=90°$ it was parallel.

The measured experimental results for the relaxation rates for the three orientations are shown in Fig. 2. Long relaxation times of over 2000 s are observed at room temperature. The results indicate the presence of a background signal due to paramagnetic impurities which must be subtracted from the observed behavior. The resulting relaxation rates are now plotted in Figs. 3–5 for $\theta=90°$,

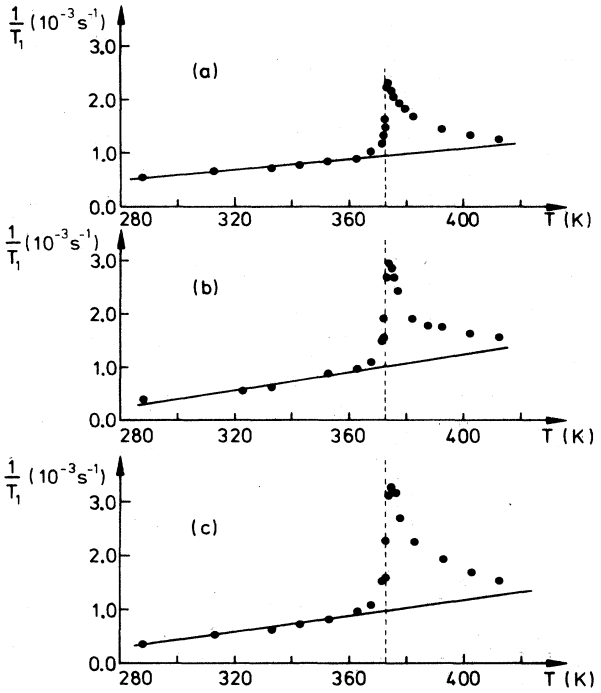

FIG. 2. T_1^{-1} as a function of temperature for three orientations of the magnetic field B_0 with respect to the b axis: (a) $\theta=0°$, (b) $\theta=54.7°$, and (c) $\theta=90°$. The solid straight line corresponds to the background relaxation.

54.7°, and 0°, respectively.

Let us now calculate T_1^{-1} from the equations given in the last section. The inputs required for this purpose are J_1, J_2, J_3, $\langle\sigma\rangle$, $D(\equiv E)$, $DE(q)$, and τ. The quantities J_2/J_1 and $|J_3|/J_1$ were recently obtained from a least-squares fit of the neutron scattering data by Ehrhardt *et al.*[14] These are $J_2/J_1=0.02$ and $|J_3|/J_1=0.001$

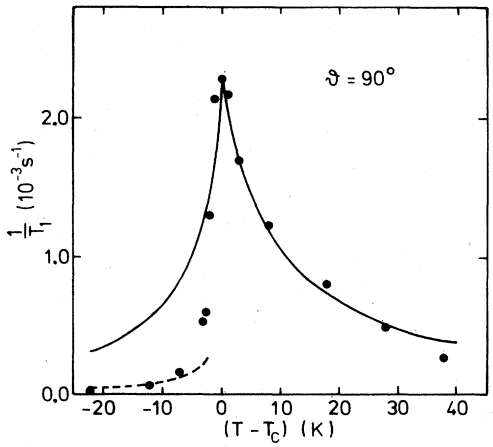

FIG. 3. T_1^{-1} as a function of $T-T_c$ for $\theta=90°$ where $T_c=375$ K. The solid curve is obtained from theoretical calculations with $J_2/J_1=0.02$, $|J_3|/J_1=0.0006$, and $\tau=1.65\times10^{-13}$ s while the dashed curve is obtained when (as explained in the text) the experimental values of the order parameter are used.

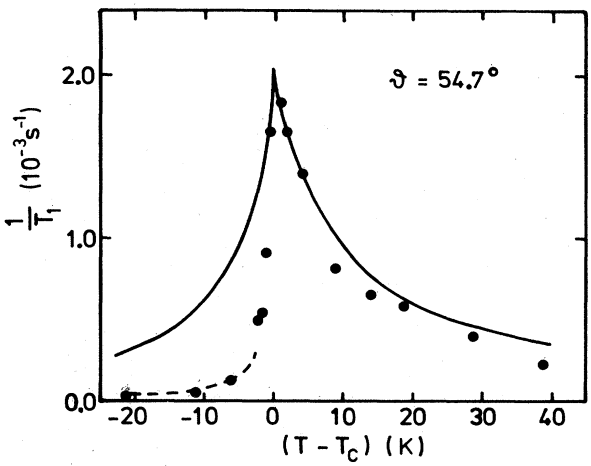

FIG. 4. Same as in Fig. 3 except $\theta=54.7°$ and $T_c=374$ K.

which give $J_1=509$ K, $J_2=10$ K, and $J_3=-0.5$ K (these differ from the values obtained from the older data[2(b)]). These values are taken as guides in our analysis. The order parameter $\langle\sigma\rangle$ is calculated from the self-consistent solution of

$$\langle\sigma\rangle=\frac{\sinh(2\beta J_\perp\langle\sigma\rangle)}{[\sinh^2(2\beta J_\perp\langle\sigma\rangle)+e^{-4\beta J_1}]^{1/2}} . \tag{17}$$

We next calculate the spectral densities which can be rewritten from Eq. (6) as

$$J^{(k)}(\omega_k)=\frac{1}{2}\sum_{\alpha=1}^{2}\int_0^1\int_0^{1-h}\int_1^2[2(D^\alpha+2DE^\alpha(q)] \times S^\alpha(h,l,k,\omega_k) \times dh\,dl\,dk . \tag{18}$$

Use has been made of the symmetry property $(h,l)\equiv(1-h,1-l)$.

The calculated values of $\tilde{D}=\frac{1}{2}\sum_\alpha D^\alpha$ for 34 nearest neighbors are listed in Table I. $\sum_\alpha DE^\alpha(q)$, on the other

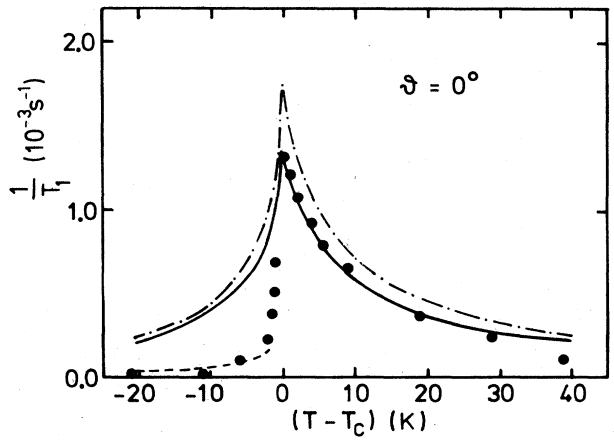

FIG. 5. Same as in Fig. 3 except that $\theta=0°$, $T_c=375$ K, and $|J_3|/J_1=0.001$. The dashed-dotted curve corresponds to $J_2/J_1=0.02$ and $|J_3|/J_1=0.0006$.

TABLE I. Lattice sums for proton dipole-dipole interaction according to Eq. (7) for three different orientations θ of the crystal b axis with respect to the external magnetic field B_0. All values are in units of 10^{-55} m^{-6}.

θ	$\tilde{D}(\omega_0)$	$\tilde{D}(2\omega_0)$
90°	0.106 50	0.311 13
54.7°	0.070 27	0.320 52
0°	0.123 88	0.190 77

hand, is q dependent and calculated for, again, 34 nearest neighbors while performing the integrations in Eq. (18).

The critical effect in the relaxation rate is thus contained in the integral $\int d^3\vec{q}s(\vec{q},\omega)$. Since

$$S(\vec{q},\omega)=\frac{2}{\beta\omega}\mathrm{Im}\chi(\vec{q},\omega)\ , \tag{19}$$

the expressions (11)—(16) can be used to evaluate $J^{(k)}(\omega_k)$. We have carried out the triple integration by Gauss quadrature formula with $n=8$. The integrals over h and l were subdivided. The convergence of the results was also checked and found good. Finally, τ is treated as a free parameter chosen such that the calculated behavior for $T>T_c$ followed closely the experimental data for all the three orientations. It should be pointed out that accurate order parameters are necessary to obtain quantitative results for $T<T_c$ in low-dimensional solids.[15]

The results shown in Fig. 3, for $\theta=90°$, were obtained using $J_2/J_1=0.02$, $|J_3|/J_1=0.0006$ ($J_1=520$ K, $J_2=10.4$ K, and $J_3=-0.3$ K), and $\tau=1.65\times10^{-13}$ s. These values were chosen such that the relaxation behavior above the critical temperature is reproduced. As is clear from the results, excellent agreement is found. For $T<T_c$, however, the agreement seems only qualitative which is due to poor estimates for the order parameter $\langle\sigma\rangle$. When experimental values of $\langle\sigma\rangle$ obtained from ^{13}C line separations[5] are used in our calculations, quantitative results (dashed curve) are again obtained. Similarly for the second orientation ($\theta=54.7°$) the results of the model, with the same set of parameters J_1, J_2, J_3, and τ, are in quantitative agreement with the experiment (Fig. 4). However, for $\theta=0°$, the above values for J_1, J_2, J_3, and τ give relaxation rates larger than the corresponding experimental values at all temperatures. We therefore studied the dependence of T_1^{-1} on J_2, J_3, and τ and found that the correct relaxation behavior can only be obtained if $|J_3|/J_1=0.001$. The results in Fig. 4 shown by the continuous line correspond to $J_2/J_1=0.02$, $|J_3|/J_1=0.0006$, and $\tau=1.65\times10^{-13}$ s while those shown by the dashed-dotted line correspond to $J_2/J_1=0.02$, $|J_3|/J_1=0.001$, and $\tau=1.65\times10^{-13}$ s. In general, we find that the results are much more susceptible to change on J_3 than to J_2 or τ. This points out the necessity of making modifications, particularly in the interchain interactions, to obtain quantitative results from the molecular-field approach.

The values of J_2/J_1 in all three orientations are the same and equal to that obtained from the neutron scattering data, while $|J_3|/J_1$, except for $\theta=0°$ orientation, are different from the neutron scattering value by a factor

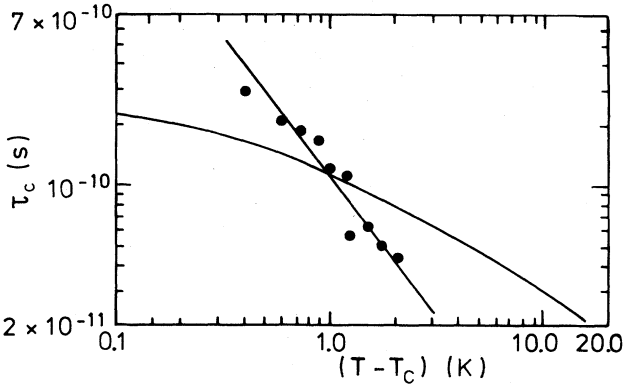

FIG. 6. Correlation time τ_c as defined in the text versus temperature above the phase transition. The straight line through the closed circles corresponds to the correlation time τ_c from the ^{13}C relaxation data (Ref. 16).

1.67. Since J_2/J_1 and $|J_3|/J_1$ have been obtained independently of the neutron scattering results, the agreement between the two is quite satisfying. The value of τ is different by 1 order of magnitude from that obtained from ^{13}C spin-lattice relaxation measurements. Note, however, that the absolute value of τ as determined from spin-lattice relaxation data is extremely sensitive to the amplitude (Δx) of the proton motion in the hydrogen bond. Since this amplitude is not known accurately enough, the absolute value of τ might be somewhat in error.

In order to furnish some quantitative insight into the critical slowing down near the phase transition we have plotted in Fig. 6 the correlation time τ_c, defined as

$$\tau_c\equiv\int_0^\infty dt\, g(t)=\int d^3\vec{q}S(\vec{q},0) \tag{20}$$

versus temperature, as obtained from the proton T_1 data using the Ising-chain analysis. The correlations are seen to decay very slowly with increasing temperature, a behavior typical for low-dimensional solids. For comparison we have also included the ^{13}C relaxation data. Note that the absolute values of ^{13}C and ^{1}H correlation time τ_c agree near the phase transition. However, with increasing temperature a deviation is observed, most likely due to the overestimated one-dimensional character of the pseudo one-dimensional kinetic Ising model.

Assuming the scaling behavior $\tau_c=\tau\epsilon^{-\lambda}$, where $\epsilon=(T-T_c)/T_c$, it is found that the data cannot be fitted with a single value of λ. If one is willing to accept for a moment a piecewise exponential law, the critical exponent λ is equal to 0.89 at $(T-T_c)=0.1$ K and then it increases progressively with temperature. For three-dimensional models[17] λ varies between 0.5 and 1.0 while for the two-dimensional Ising lattice it is 1.6 (Ref. 18). The experimental behavior might thus indicate the existence of three-dimensional fluctuations near the phase-transition region which become increasingly lower dimensional with an increase in temperature, i.e., the phase transition is essentially driven by three-dimensional fluctuations. This situation is similar to low-dimensional magnetic systems where the phase transition is a three-

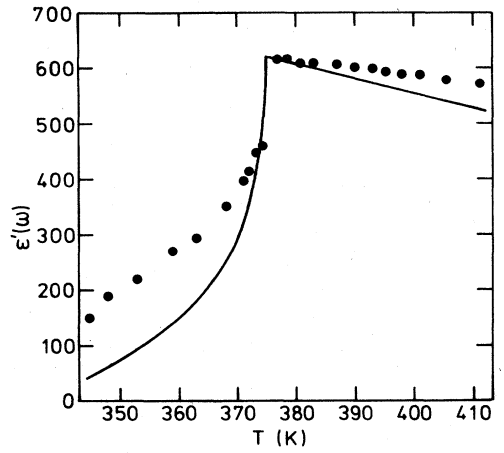

FIG. 7. Dielectric susceptibility versus temperature. The experimental points were obtained from Ref. 20 and are compared with our calculation (solid line) based on the Ising chain model [Eq. (23a)].

dimensional ordering process and, for example, one-dimensional fluctuations are observed in the paramagnetic ($T > T_c$) region. Such a behavior is indeed expected from the structure and the type of interactions present in $H_2C_4O_4$. In essence this behavior is built into our model.

Within our model of kinetic Ising chains, we are also able to calculate the dielectric susceptibility

$$\epsilon(\omega)=1+4\pi\chi(q=0,\omega) , \tag{21}$$

where

$$\epsilon(\omega)=\epsilon'(\omega)-i\epsilon''(\omega) . \tag{22}$$

When using Eq. (11) we arrive at

$$\epsilon'(\omega)=1+\frac{4\pi\chi(\omega,0)}{1+\omega^2\tau_0^2} , \tag{23a}$$

$$\epsilon''(\omega)=4\pi\frac{\omega\tau_0\chi(\omega,0)}{1+\omega^2\tau_0^2} . \tag{23b}$$

The real part $\epsilon'(\omega)$ has been measured by Feder[19] and Maier *et al.*[20] at low frequencies. We compare their results with our calculation based on Eq. (23a) together with Eqs. (12)—(16) in Fig. 7.

ACKNOWLEDGMENTS

We would like to thank J. Petersson and U. Buchenau for enlightening discussions. We gratefully acknowledge financial support by the Stiftung Volkswagenwerk. One of us (P.K.K.) thanks the Alexander von Humboldt-Stiftung for financial support.

*Present address: Mathematischer Beratungs- und Programmierungsdienst GmbH, Semerteichstrasse, 4600 Dortmund 1, Federal Republic of Germany.

†Present address: Siemens, Medizinische Technik, 8520 Erlangen, Federal Republic of Germany.

[1]D. Semmingsen and J. Feder, Solid State Commun. **15**, 1369 (1974).

[2](a) E. J. Samuelsen and D. Semmingsen, Solid State Commun. **17**, 217 (1975); (b) J. Phys. Chem. Solids **38**, 1275 (1977).

[3]W. Kuhn, H. D. Maier, and J. Petersson, Solid State Commun. **32**, 249 (1979).

[4]M. Mehring and D. Suwelack, Phys. Rev. Lett. **42**, 317 (1979).

[5]M. Mehring and J. D. Becker, Phys. Rev. Lett. **47**, 366 (1981).

[6]U. Deininghaus and M. Mehring, Solid State Commun. **39**, 1257 (1981).

[7]R. Blinc, S. Žumer, and G. Lahajnar, Phys. Rev. B **1**, 4456 (1970).

[8]R. Blinc, B. Žekš, A. Levstik, C. Filipič, J. Slak, M. Burgar, I. Zupančič, L. A. Shuvalov, and A. I. Baranov, Phys. Rev. Lett. **43**, 231 (1979).

[9]B. Topič, V. Rutar, J. Slak, M. I. Burgar, S. Žumer, and R. Blinc, Phys. Rev. B **21**, 2695 (1980).

[10]S. Žumer, Phys. Rev. B **21**, 1298 (1980).

[11]H. D. Maier, H. E. Müser, and J. Petersson, Z. Phys. B **46**, 251 (1981).

[12]H. D. Maier and J. Petersson, Solid State Commun. **45**, 175 (1983).

[13]A. Abragam, *The Principles of Nuclear Magnetism* (Oxford University Press, London, 1961).

[14]K.-D. Ehrhardt, U. Buchenau, E. J. Samuelsen, and H. D. Maier, Phys. Rev. B **29**, 996 (1984).

[15]E. R. Mognaschi, A. Rigamonti, and L. Menafra, Phys. Rev. B **14**, 2005 (1976).

[16]S. Suwelack and M. Mehring, Solid State Commun. **33**, 207 (1980).

[17]H. E. Stanley, *Introduction to Phase Transitions and Critical Phenomena* (Clarendon, Oxford, 1971).

[18]E. Stoll, K. Binder, and T. Schneider, Phys. Rev. B **8**, 3266 (1973).

[19]J. Feder, Ferroelectrics **12**, 71 (1976).

[20]H. D. Maier, D. Müller, and J. Petersson, Phys. Status Solidi B **89**, 587 (1978).